Journal of Petroleum Science and Engineering 210 (2022) 110056

Contents lists available at ScienceDirect

Journal of Petroleum Science and Engineering

journal homepage: www.elsevier.com/locate/petrol

Oil-source correlation under the complex geological conditions: A case study of the Chaiwopu Sag, southern Junggar Basin, NW China

Ruihui Zheng [a,b], Guanlong Zhang [c], Yansheng Qu [c], Shengzhu Wang [c], Xiao Jin [a,b,d], Xue Chen [a,b], Zhihuan Zhang [a,b,*]

[a] College of Geosciences, China University of Petroleum, Beijing, 102249, China
[b] State Key Laboratory of Petroleum Resources and Prospecting, China University of Petroleum, Beijing, 102249, China
[c] Exploration and Development Research Institute of Shengli Oilfield, SINOPEC, Dongying, Shandong, 257061, China
[d] Development and Research Center, National Geological Archives of China, China Geological Survey, Beijing, 100037, China

ARTICLE INFO

Keywords:
Unconventional resource
Biodegradation
Hydrocarbon inclusion
Carbon isotope
Oil-source correlation

ABSTRACT

Slightly (PM 1) to very strongly (PM 9) biodegraded crude oil was discovered in the reservoir of the Tashikula Formation in the eastern Chaiwopu Sag. The origin of oil in the eastern Chaiwopu Sag remains unclear due to different degrees of biodegradation and multi-stage nappe structure. In this study, the geochemical data from crude oil, source rocks and hydrocarbon inclusions are used to establish the correlations between oils and source rocks under complex geological conditions. The characteristics of biomarkers, isotopes and hydrocarbon inclusions reveal two stages of hydrocarbon charging in the eastern Chaiwopu Sag. Hydrocarbons formed during the first charging stage has low maturity and a relatively light carbon isotope composition, and its relative abundance of C_{20-23} tricyclic terpanes follows the sequence: $C_{23} > C_{21} > C_{20}$. Hydrocarbons formed during the second charging stage is characterized by relatively high maturity and heavy carbon isotope composition, and the corresponding abundance of C_{20-23} tricyclic terpanes is $C_{23} < C_{21} < C_{20}$. The biomarkers and isotopic characteristics of crude oil, source rocks and hydrocarbon inclusions reveal the hydrocarbons formed during the first charging stage originated from the Lucaogou Formation in the northern Chaiwopu Sag and the northern Bogeda Mountains, and those formed during the second charging stage originated from the Lucaogou Formation in the central Chaiwopu Sag. The high-quality source rocks and reservoirs of the Lucaogou Formation were deposited in the northern Chaiwopu Sag, which has great potential for tight/shale oil exploration.

1. Introduction

The Chaiwopu Sag, located in the southeastern Junggar Basin, is an important exploration target for shale/tight oil (Guo, 1997; Wu et al., 2003; Guo et al., 2004, 2006; Kuang et al., 2005; Li, 2006; Fan, 2018). The Chaiwopu Sag is surrounded by the Bogeda Mountains in the northeast and the Habirga Mountains in the south (Fig. 1). The reverse faults developed in the Sag complicate petroleum exploration. Due to the complex accumulation history of the reservoir and the variable effect of secondary alteration processes, a single research method often fails to produce rational interpretations.

Biomarker compounds and carbon isotope compositions of hydrocarbons mainly reflect information of the original organic matter, so they are widely used in oil-source and oil-oil correlation studies (Stahl and Carey, 1975; Gratzer et al., 2011; Mashhadi and Rabbani, 2015; Alizadeh et al., 2018; Wu et al., 2020; Körmös et al., 2021). Both light and heavy crude oils were discovered in the eastern Chaiwopu Sag, indicating that there may be different degrees of biodegraded crude oil in this area. Biodegradation changes the physical and chemical properties of crude oil, leading to misinterpretation of petroleum geochemical analyses (Seifert et al., 1984; Peters and Moldowan, 1993; Wenger et al., 2002; Peters et al., 2005). Thus, accurate evaluation of biodegradation is of great significance for petroleum geochemical analyses. The biodegradation of crude oil shows a specific sequence, and the PM scale proposed by Peters and Moldowan (1993) is widely used to classify the biodegradation level of crude oil. According to appearance, alteration or disappearance of *n*-alkanes, hopanes and steranes, the biodegradation level of crude oil can be divided into level 1 (least altered) to level 10 (most altered).

Fluid inclusions comprise oil inclusions, gas inclusions and aqueous

* Corresponding author. College of Geosciences, China University of Petroleum, Beijing, 102249, China.
E-mail address: zhangzh3996@vip163.com (Z. Zhang).

https://doi.org/10.1016/j.petrol.2021.110056
Received 26 May 2021; Received in revised form 21 November 2021; Accepted 14 December 2021
Available online 16 December 2021

inclusions. Fluid inclusions are closed systems, the volume of fluid remains unchanged and is not affected by temperature (Goldstein, 2001; Pironon, 2004). By analyzing the fluorescence characteristics and homogenization temperature of fluid inclusions, as well as the composition of hydrocarbon inclusions, we can derive their composition and temperature at the time of capture. According to those data, its origin (Volk et al., 2000; Parnell et al., 2001; Liu and Eadington, 2005), migration and accumulation (McLimans, 1987; Tseng and Pottorf, 2003; Duschl et al., 2016) of petroleum can be revealed. Moreover, fluid inclusions are used to study the thermodynamic properties and composition of hydrocarbons (Ruble et al., 1998; Aplin et al., 1999; Thiéry et al., 2002; Ryder et al., 2004; Liu et al., 2007; Volk and George, 2019). Therefore, fluid inclusions play an important role in petroleum geology and organic geochemistry (George et al., 2001; Zhao et al., 2019).

The organic-rich source rocks of the Permian, Triassic and Jurassic were discovered in the Sag. Among them, the Middle Permian Lucaogou Formation is an important lacustrine source rock in the Chaiwopu Sag, and the characteristics of crude oil and the Lucaogou Formation source rocks in the western and central sags have been clearly defined (Guo, (1997); Wu et al., (2003); Kuang et al., (2005); Li, (2006); Guo et al., (2006a), (2006b)). However, due to different degrees of crude oil degradation and lack of exploratory wells, there are few studies on crude oil characteristics and oil-source correlation in the eastern Chaiwopu Sag. Based on the analysis of geochemical characteristics of crude oil and source rocks, this paper studies the oil-source correlation in the eastern Chaiwopu Sag based mostly on biomarker data, carbon isotopes and fluid inclusions. The results suggest that comprehensive use of biomarkers, carbon isotopes and fluid inclusions for oil-source correlation study can provide a new insight into oil-source correlation research under complex geological conditions.

2. Geological background

The Chaiwopu Sag is a Paleozoic-Cenozoic intermontane, superimposed sag in the southeastern Junggar Basin covering an area of about 3683.7 km^2. The Sag is surrounded by the Bogeda Mountains in the northeast, the Habirga Mountains in the south and the Northern Tianshan Mountains in the northwest (Fig. 1). The Sag can be further divided into the Yongfeng Subsag, the Sangezhuang Uplift and the Dabancheng Subsag (Fig. 1). Affected by the uplift of the Bogeda Mountains and the Habirga Mountains, the strata are strongly deformed and multi-stage nappe structures are developed in the eastern Chaiwopu Sag (Fig. 2).

Since the deposition of the Carboniferous sedimentary strata, the sedimentations, in the south of the Bogeda region, have been affected by late Hercynian Events, Indosinian Events, Yanshan Events and Himalayan Events. During the Middle Permian, lacustrine sediments were deposited with organic-rich sediments formed in the Lucaogou Formation, which are the most important source rocks in this Sag (Li, 2006). The Sag was affected by the tectonic movement of the North Tianshan Mountains during the Middle Permian, and sedimentary facies evolved from lacustrine into swamp-flood plains-delta facies in the study area. The superposition of multiple structural movements formed the current tectonic framework of the Chaiwopu Sag.

The stratigraphic section of the area includes a series of formations ranging in age from Carboniferous to Quaternary. The Lower Permian strata contain the Shirenzigou (P_1sh) and Tashikula (P_1t) Formations, the Middle Permian strata comprise the Wuerhe (P_2w), Jingjingzigou (P_2j), Lucaogou (P_2l) and Hongyanchi (P_2h) Formations. The Lucaogou Formation mainly consists of organic-rich shale, mudstone, dolomitic limestone and sandstone (Table 1).

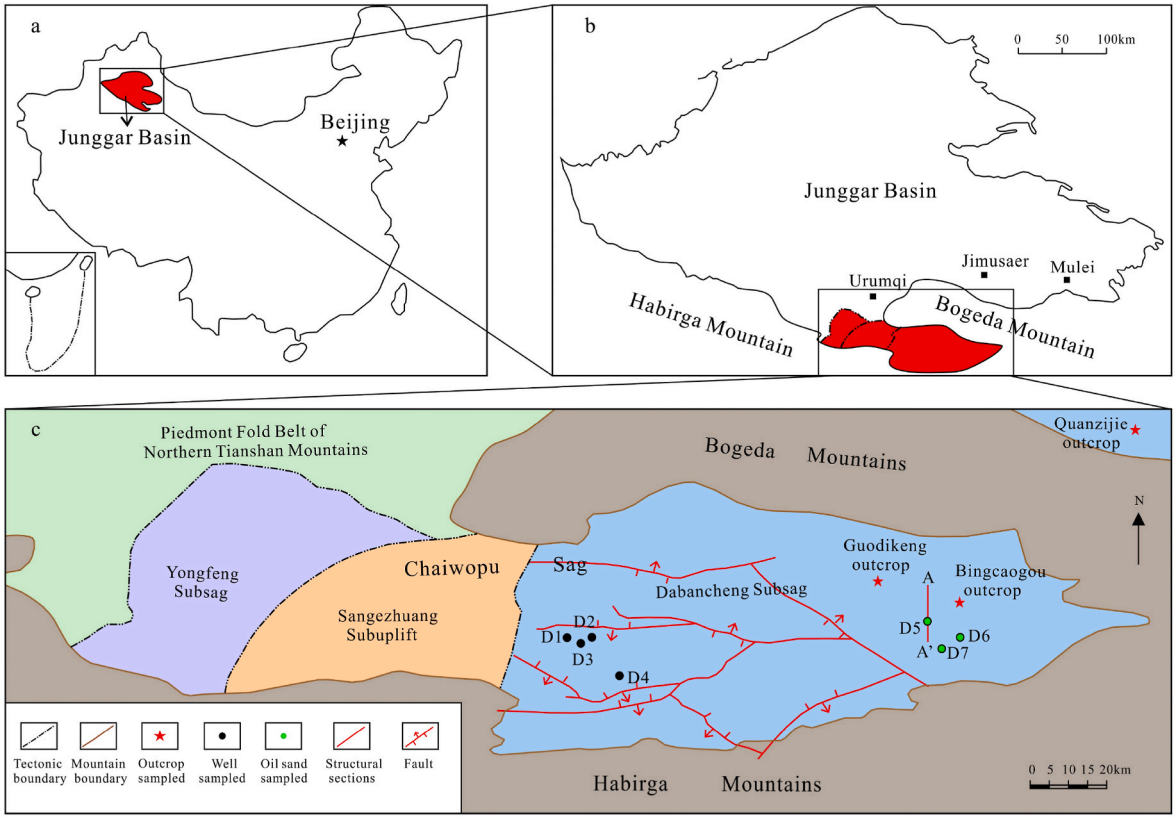

Fig. 1. Location and geological sketch of the study area. (a) The Junggar Basin in China (from Hu et al., 2018); (b) The study area in Junggar Basin (modified from Hu et al., 2018); (c) Structural units and sample collection locations in the Chaiwopu Sag.

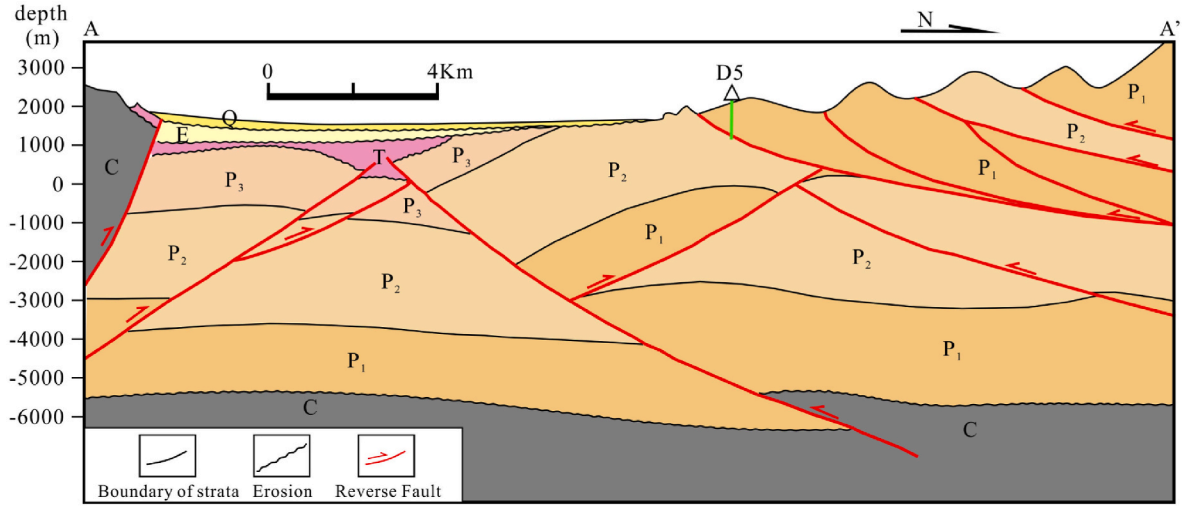

Fig. 2. The structural section in the eastern Chaiwopu Sag (see Fig.1c).

Table 1
Summary of Permian strata in the study area (from Li, 2006).

Lithostratigraphy		Lithostratigraphy			
System	Group	Formation	Code	Thickness/m	Lithology
Permian	Xiacangfanggou	Guodikeng	P_3g	1653	Mudstone, silty mudstone, sandstone, gravel-bearing sandstone
		Wutonggou	P_3w		
		Quanzijie	P_3q		Reddish-brown conglomerate, sandy mudstone, sandstone, mudstone, carbonaceous mudstone, coal line
	Shangjijigoucao	Hongyanchi	P_2h	728	Grey-green mudstone, grey-black mudstone, carbonaceous mudstone, sandstone
		Lucaogou	P_2l	650	Grey-green shale, grey-black shale, oil shale, mudstone, dolomitic limstone, sandstone
		Jingjingzigou	P_2j	235	Grey tuff, quartz sandstone, sandy mudstone, black mudstone
		Wuerhe	P_2w	300	Grey-green conglomerate, quartz sandstone, tuffaceous sandstone, grey mudstone
	Xiajijigoucao	Tashenkula	P_1t	374	Grey-green sandstone, quartz sandstone, sandy mudstone, black mudstone
		Shirenzigou	P_1sh	91	Grey sandstone and siltstone, dark grey and black mudstone, calcareous mudstone

3. Samples and experimental methods

3.1. Samples

Fifty-eight core and outcrop samples of P_2l were analyzed for TOC and S_1+S_2 (hydrocarbon-generation potential), and eighteen core and outcrop samples were analyzed for maturity. The saturated hydrocarbon biomarkers and the carbon isotopic compositions of extracts from 20 core and outcrop mudstone samples and 4 oil-bearing siltstone samples were analyzed (Table 2). Additionally, the saturated hydrocarbon biomarkers in inclusions from two oil-bearing siltstone samples were analyzed by GC-MS. Sample information is shown in Fig. 1 and Table 2.

3.2. Experimental methods

3.2.1. Quality analysis and pretreatment of source rock samples

The TOC analyses were conducted on a LECO CS-230 instrument, and the S_1+S_2 analyses were conducted on a Rock-Eval-II instrument. These samples were first crushed and sieved to 150 μm, and then directly used for the S_1+S_2 analysis. The following treatments are required before the TOC analysis of these samples: firstly, the carbonate minerals were removed with 5% HCl at 80 °C, and the residual HCl was washed away with distilled water. Then, these samples were dried at 70 °C for 10 h.

The vitrinite reflectance (Ro) of the sample was measured on a Lecia DM500 microscope equipped with a 50-X oil-immersion objective lens under reflected light. First, the rock sample was mixed with hardener and epoxy resin to prepare a column, and then the prepared sample was cut and polished. According to the People Republic of China petroleum natural gas profession standard (SY/T 5124–2012), the Ro of sample was measured, and the Ro value represents the average value of at least 30 points.

The 150 μm fraction of the source rock sample was extracted using dichloromethane and methanol (93:7, v:v; 48 h of continuous extraction at a constant temperature of 60 °C in a Soxhlet apparatus). Petroleum ether was added to 20–30 mg of the extract and the insoluble fraction was asphaltene. The soluble fraction was fractionated into saturated hydrocarbons, aromatic hydrocarbons and polar compounds through column chromatography with alumina/silica gel (2:3) as the stationary phase. The saturated hydrocarbons were eluted using petroleum ether (40 mL), aromatic hydrocarbons using petroleum ether/dichloromethane (v:v = 1:2, 30 mL) and dichloromethane (20 mL) for polar

Table 2
Location and numbers of mudstones and oil-sand samples in the Chawiopu Sag.

Formation (Fm)	Mudstones and numbers							Oil-sand and numbers		
	D1	D2	D3	D4	Guodikeng	Bingcaogou	Quanzijie	D5	D6	D7
Lucaogou.Fm(P_2l)	10	4	3	6	9	16	10	/	/	/
Tashikula.Fm(P_1t)	/	/	/	/	/	/	/	1	2	1

compounds. Samples were analyzed for biomarkers using gas chromatography-mass spectrometry (GC-MS).

3.2.2. Biomarker characteristics of mudstone and oil sand extracts

The GC-MS analysis of saturated hydrocarbon fractions was conducted on an Agilent 5975i Mass Spectrometer, coupled with an Agilent 6890 Gas Chromatography equipped with a HP-5MS column (length: 30 m, diameter: 0.25 mm; film thickness: 0.25 μm). Helium was used as the carrier gas with an average velocity of 36 cm/s. The initial temperature of the GC oven was set to 50 °C, then heated to 310 °C at the rate of 3 °C/min, and finally kept isothermal for 20 min. The ionization mode of electron impact was adopted, and the ionization energy is 70 eV.

3.2.3. Geochemical analysis of hydrocarbon inclusions

Based on petrographic research, samples with a high abundance of hydrocarbons and only one-stage of hydrocarbon inclusions were selected to be crushed to 60–90 μm and extracted using the Soxhlet apparatus ($V_{dichloromethane}$: $V_{methanol}$ = 93:7, 48 h of continuous extraction at a constant temperature of 60 °C): this treatment is used to remove the absorbed hydrocarbons from pores and particle surfaces. Then, carbonate minerals were removed with 10% HCl. The second Soxhlet extraction ($V_{dichloromethane}$: $V_{methanol}$ = 93:7, 48 h, 60 °C) was carried out after removing the carbonate minerals. The second extracted particles were treated with chromic acid ($K_2Cr_2O_7$:H_2SO_4) to remove oxidized residue and frequently stirred with a glass rod. The third Soxhlet extraction ($V_{dichloromethane}$: $V_{methanol}$ = 93:7, 48 h, 60 °C) was carried out after removing the oxidized residue: this treatment is used to fully remove any absorbed hydrocarbons from pores and particle surfaces. The GC-MS analysis results of the third extract were compared with the blank group, if there were compounds, the above treatments were repeated. Finally, these treated samples were powdered to liberate hydrocarbons from inclusions in a sealed vacuum tank. The hydrocarbons from inclusions were obtained by ultrasonic extraction (dichloromethane). The saturated hydrocarbon biomarkers were detected by the GC-MS. The experimental conditions are the same as 3.2.2.

3.2.4. Stable carbon isotope

The carbon isotope analysis of extracted fractions (asphaltenes, saturated and aromatic hydrocarbons, polar compounds) was conducted on a Thermo MAT-253 isotope ratio mass spectrometer connected to a Flash EA 2000 elemental analyzer. The carrier gas was helium and high purity oxygen was the combustion gas. The filling material of the reactor is composed of chromium oxide, copper and silver-bearing cobalt oxide. The temperature of the reactor is 980 °C.The testing standard is SY/T 5238–2019. During sample analysis, a parallel sample was added every 10 samples, and the analysis error of the parallel sample is less than ±5‰.

3.2.5. Measures of ensuring samples analyzing quality

All the organic solvents in the experiment were analytically pure, distilled by the Soxhlet apparatus and tested with GC-MS. The silica (150–300 μm) was extracted until it no longer fluoresced before being activated at 150 °C for 8 h. The alumina extracted and activated at 450 °C for 8 h. Then, both silica and alumina were stored in a dryer. Identification of saturated hydrocarbon compounds was achieved by matching characteristic ions and their retention times with those of authentic standard. In addition, the purity of the carrier gas used in the experimental analysis was higher than 99.999%. The filling materials in experiments, such as chromium oxide and copper, are in line with the international quality standard system ISO9001 certification.

4. Results and discussion

4.1. Geochemical analysis of potential source rocks

4.1.1. Source rocks in the central Chaiwopu Sag

Twenty-three core mudstones of P_2l form the central Chaiwopu Sag (Table 2) were selected for geochemical analysis, and these samples came from wells D1, D2, D3 and D4 (Fig. 1c).

The total sedimentary thickness of P_2l in the central Chaiwopu Sag is over 200.0 m, and the cumulative thickness of mudstone is approximately 100.0 m. The P_2l was deposited in a fan delta front subfacies. The TOC and S_1+S_2 values of mudstones range from 0.03 to 0.35% (mean = 0.13%) and 0.01–0.54 mg/g (mean = 0.08 mg/g), respectively (Table 3 and Fig. 3a). According to the cross plot of HI vs. Tmax, the organic matter mainly belongs to type II_2 and III (Fig. 3b). Ro varies from 0.82 to 1.68% (mean = 1.29%, Table 3). The above results show that the mudstones are organic lean with high maturity, and correspond to the wet gas zone.

The saturated hydrocarbon biomarkers of the P_2l mudstone in wells D1 and D2 are different from that in the northern Chaiwopu Sag and the northern Bogeda Mountains, as shown in Fig. 4a and b. Specifically, the geochemical characteristics of biomarkers in mudstone are as follows: (i) High amount of short-chain *n*-alkanes, except for the sample from well D1, which contains more long-chain *n*-alkanes (Fig. 4b). (ii) The abundance of tricyclic terpanes is higher than that of pentacyclic triterpenes, and the abundance of the C_{20}-, C_{21}- tricyclic terpanes is relatively high. (iii) The abundance of pregnane and homopregnane is higher than that of regular steranes (Fig. 4a and b). The G/C_{30}H ratio is between 0.15 and 0.19 (Table 3). Tricyclic terpanes with a carbon number less than C_{21} come from terrigenous higher plants (Zumberge, (1987); Zhu, (1997)). The low G/C_{30}H value and high abundance short-chain in tricyclic terpanes suggest that the mudstone is deposited in a freshwater environment and the origin of organic matter is mainly composed of terrestrial higher plants.

4.1.2. Source rocks in the northern Chaiwopu Sag

Twenty-five outcrop shales of P_2l in the northern Chaiwopu Sag (Table 2) were selected for geochemical analyses, and these samples came from the outcrop profiles of Guodikeng and Bingcaogou (Fig. 1c).

The P_2l source rock in the northern Chaiwopu Sag is composed of black shale. The TOC of the source rock ranges from 0.27 to 5.90% (mean = 1.76%), and the S_1+S_2 values range from 0.05 to 27.84 mg/g (mean = 7.18 mg/g) (Table 3 and Fig. 3a). According to the cross plot of HI vs Tmax, the organic matter of black shale mainly belongs to typeI, type II_1 and type III (Fig. 3b). Ro varies from 0.76 to 0.85% (mean = 0.81%, Table 3), indicating that the source rock has a moderate maturity and corresponds to the oil window zone. These evaluation parameters, such as the TOC and S_1+S_2, indicating that most shale samples were classified as fair-very good source rocks for petroleum generation (Fig. 3a), which is favorable for generating petroleum.

The biomarker compositions of P_2l source rock in the Guodikeng outcrop are shown in Fig. 4c. Specifically, the geochemical characteristics of biomarkers in the shale are as follows: (i) The content of long-chain is high in *n*-alkanes. (ii) The abundance of pentacyclic triterpenes is higher than that of tricyclic terpanes, and the relative abundance of the $C_{20\text{-}23}$ tricyclic terpanes has the characteristics of C_{23}> C_{21}> C_{20}. (iii) The regular steranes are more abundant than pregnane and homopregnane. The G/C_{30}H and C_{27}/C_{29}-regular steranes rations range from 0.39 to 0.57 and 0.15 to 0.32 (Table 3), respectively. High G/C_{30}H value and high abundance of C_{29}-regular steranes suggest that the shale is deposited in a salt water environment and the organic matter is mainly originated from terrestrial higher plants.

4.1.3. Source rocks in the northern Bogeda Mountains

Ten outcrop shale samples of P_2l from the northern Bogeda Mountains (Table 2) were chosen for geochemical analysis, and these samples

Table 3
Geochemical parameters and biomarker parameters of the P_2l source rocks in different areas.

Well/outcrop	Depth (m)	TOC (%)	S_1(mg/g)	S_2(mg/g)	S_1+S_2 (mg/g)	Tmax(°C)	HI (mg/g)	Ro (%)	G/C_{30}H	C_{27}/C_{29}-RST
D1	2637	0.16	0.01	0.03	0.04	486	18.69	\	\	\
D1	2725	0.13	0.01	0.09	0.10	434	69.66	0.85	0.16	0.53
D1	2726	0.11	0	0.02	0.02	506	18.20	\	\	\
D1	2731	0.09	0	0.01	0.01	490	10.54	0.92	0.19	0.59
D1	2733	0.03	0.02	0.02	0.04	474	59.35	\	\	\
D1	2735	0.08	0.02	0.03	0.05	464	35.42	\	\	\
D1	2738	0.14	0.08	0.09	0.17	441	64.29	0.94	\	\
D1	2741	0.16	0.06	0.04	0.10	488	25.00	\	\	\
D1	2745	0.35	0.29	0.25	0.54	356	72.05	1.06	\	\
D1	2746	0.09	0.04	0.04	0.08	461	44.30	\	\	\
D2	3052	0.21	0.01	0.03	0.04	282	14.43	1.35	0.15	0.45
D2	3062	0.07	0.01	0.02	0.03	476	29.82	\	0.16	0.42
D2	3282	0.07	0.01	0.02	0.03	331	28.85	1.42	0.18	0.45
D2	3046	0.10	0.02	0.05	0.07	423	50.57	\	\	\
D3	3780	0.24	0.07	0.47	0.54	435	195.83	\	\	\
D3	3785	0.13	0.03	0.04	0.07	483	22.90	1.32	\	\
D3	3788	0.07	0.02	0..04	0.06	485	27.25	1.35	\	\
D3	3810	0.17	0.02	0.07	0.09	481	24.24	1.48	\	\
D3	3821	0.27	0.01	0.03	0.04	482	11.15	\	\	\
D3	3830	0.10	0.01	0.02	0.03	476	19.80	1.49	\	\
D4	3056	0.07	0.01	0.03	0.04	487	40.61	1.41	0.15	0.45
D4	3057	0.10	0.04	0.05	0.09	490	51.75	1.46	0.16	0.43
D4	3058	0.13	0.02	0.04	0.06	487	30.82	1.68	0.15	0.46
Guodikeng	\	0.63	0.03	0.14	0.17	445	22.34	\	\	\
Guodikeng	\	3.60	0.23	27.61	27.84	441	767.37	0.82	0.39	0.15
Guodikeng	\	0.42	0.04	0.11	0.15	437	26.02	\	\	\
Guodikeng	\	3.59	0.22	22.15	22.37	438	616.65	\	0.57	0.18
Guodikeng	\	0.88	0.02	0.25	0.27	449	28.40	0.76	0.41	0.22
Guodikeng	\	0.61	0.01	0.06	0.06	491	8.16	\	\	\
Guodikeng	\	0.27	0.01	0.04	0.05	353	14.92	\	\	\
Guodikeng	\	0.94	0.01	0.26	0.27	447	27.60	0.85	0.45	0.32
Guodikeng	\	3.72	0.36	13.05	13.41	439	351.18	\	0.41	0.20
Bingcaogou	\	1.68	0.09	9.53	9.62	445	566.25	\	\	\
Bingcaogou	\	5.90	0.32	26.68	27.00	439	452.05	\	\	\
Bingcaogou	\	0.91	0.08	0.11	0.19	436	12.07	\	\	\
Bingcaogou	\	1.90	0.19	14.96	15.15	445	787.78	\	\	\
Bingcaogou	\	5.42	0.42	23.18	23.60	442	427.78	\	\	\
Bingcaogou	\	0.99	0.05	0.09	0.14	450	9.12	\	\	\
Bingcaogou	\	4.59	0.31	17.49	17.80	441	381.21	\	\	\
Bingcaogou	\	0.66	0.04	0.05	0.09	447	7.62	\	\	\
Bingcaogou	\	1.02	0.09	7.36	7.45	443	721.57	\	\	\
Bingcaogou	\	0.62	0.02	0.05	0.07	445	8.05	\	\	\
Bingcaogou	\	0.98	0.03	0.05	0.08	451	5.11	\	\	\
Bingcaogou	\	0.71	0.02	0.04	0.06	449	5.60	\	\	\
Bingcaogou	\	0.62	0.03	0.08	0.11	453	13.00	\	\	\
Bingcaogou	\	1.28	0.11	6.63	6.74	440	520.00	\	\	\
Bingcaogou	\	1.53	0.23	6.75	6.98	441	440.89	\	\	\
Bingcaogou	\	0.45	0.01	0.04	0.05	438	8.82	\	\	\
Quanzijie	\	3.49	0.21	6.62	6.83	450	189.68	\	0.21	0.34
Quanzijie	\	5.61	1.15	16.36	17.51	451	291.88	\	\	\
Quanzijie	\	3.10	0.29	5.46	5.75	447	176.24	\	0.23	0.35
Quanzijie	\	4.43	0.42	15.15	15.57	450	342.30	0.67	0.23	0.45
Quanzijie	\	9.79	0.84	73.65	74.49	445	752.53	\	\	\
Quanzijie	\	10.04	1.33	64.57	65.90	441	643.13	0.59	0.21	0.32
Quanzijie	\	5.77	0.43	27.27	27.70	453	472.78	\	\	\
Quanzijie	\	2.65	0.20	0.47	0.67	320	17.75	\	0.25	0.51
Quanzijie	\	1.48	0.25	0.55	0.80	453	37.14	\	0.26	0.48
Quanzijie	\	21.35	0.68	194.63	195.31	451	738.63	\	0.22	0.58

came from the outcrop profile of Quanzijie (Fig. 1c).

The P_2l source rock in the northern Bogeda Mountains is deposited in deep-lacustrine facies and composed of black shale. The TOC values of shales range from 1.48 to 21.35% (mean = 6.77%), the S_1+S_2 values range from 0.67 to 195.31 mg/g (mean = 41.05 mg/g) (Table 3 and Fig. 3a). According to the cross plot of HI vs Tmax, the organic matter mainly belongs to type Iand type II_1 (Fig. 3b). Ro varies from 0.59 to 0.67% (mean = 0.63%, Table 3), indicating that the maturity of the shale is relatively low and corresponds to early oil window zone. These evaluation parameters, such as the TOC and S_1+S_2, indicating that the shales were classified as good-very good source rocks for petroleum generation (Fig. 3a), which is favorable for generating petroleum.

The biomarker compositions of P_2l shale in the Quanzijie outcrop are shown in Fig. 4d and e. The distribution characteristics of biomarkers are similar to those in the northern Chaiwopu Sag, but the abundance of C_{28}-regular sterane is higher than that in the northern Chaiwopu Sag. The values of G/C_{30}H and C_{27}/C_{29}-regular steranes are 0.21–0.26 and 0.32–0.58 (Table 3), respectively. The medium G/C_{30}H and C_{27}/C_{29}-regular steranes ratios suggest that the shale is deposited in saline water and the origin of organic matter is a mixture of terrigenous and aquatic.

The carbon isotope values of extracted fractions of mudstone and shale are shown in Table 4. The extracts of shale in the Guodikeng outcrop are relatively rich in light carbon isotopes, and the extracts of mudstone and shale in other area are relatively rich in heavy carbon isotopes.

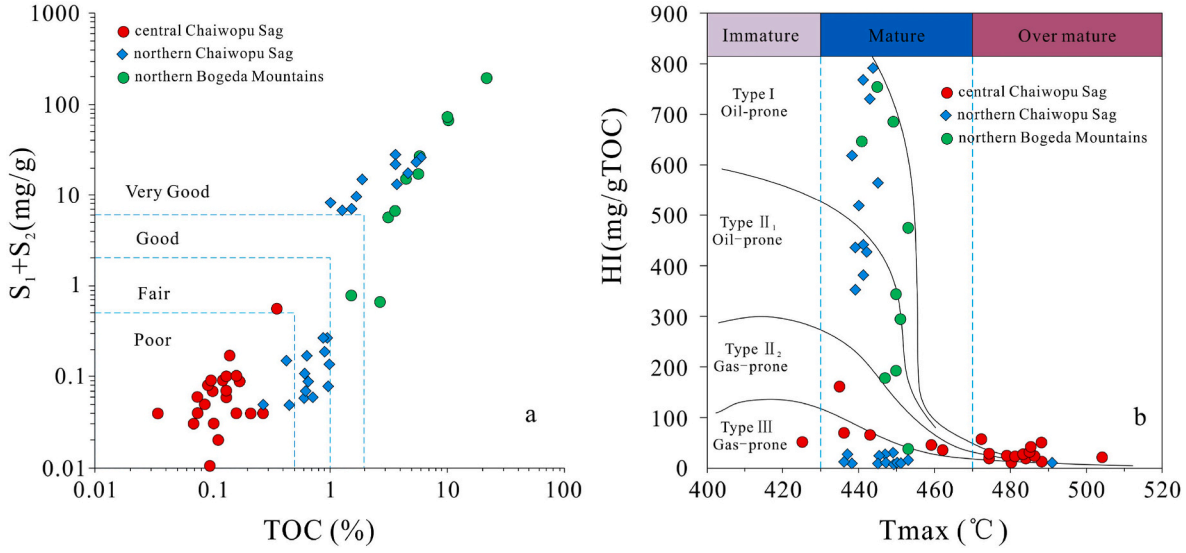

Fig. 3. Geochemical parameters intersection diagram of the P_2l source rocks in the Chaiwopu Sag and northern Bogeda Mountains. (a) S_1+S_2 vs. TOC (after Peters, 1986); (b) HI vs. Tmax.

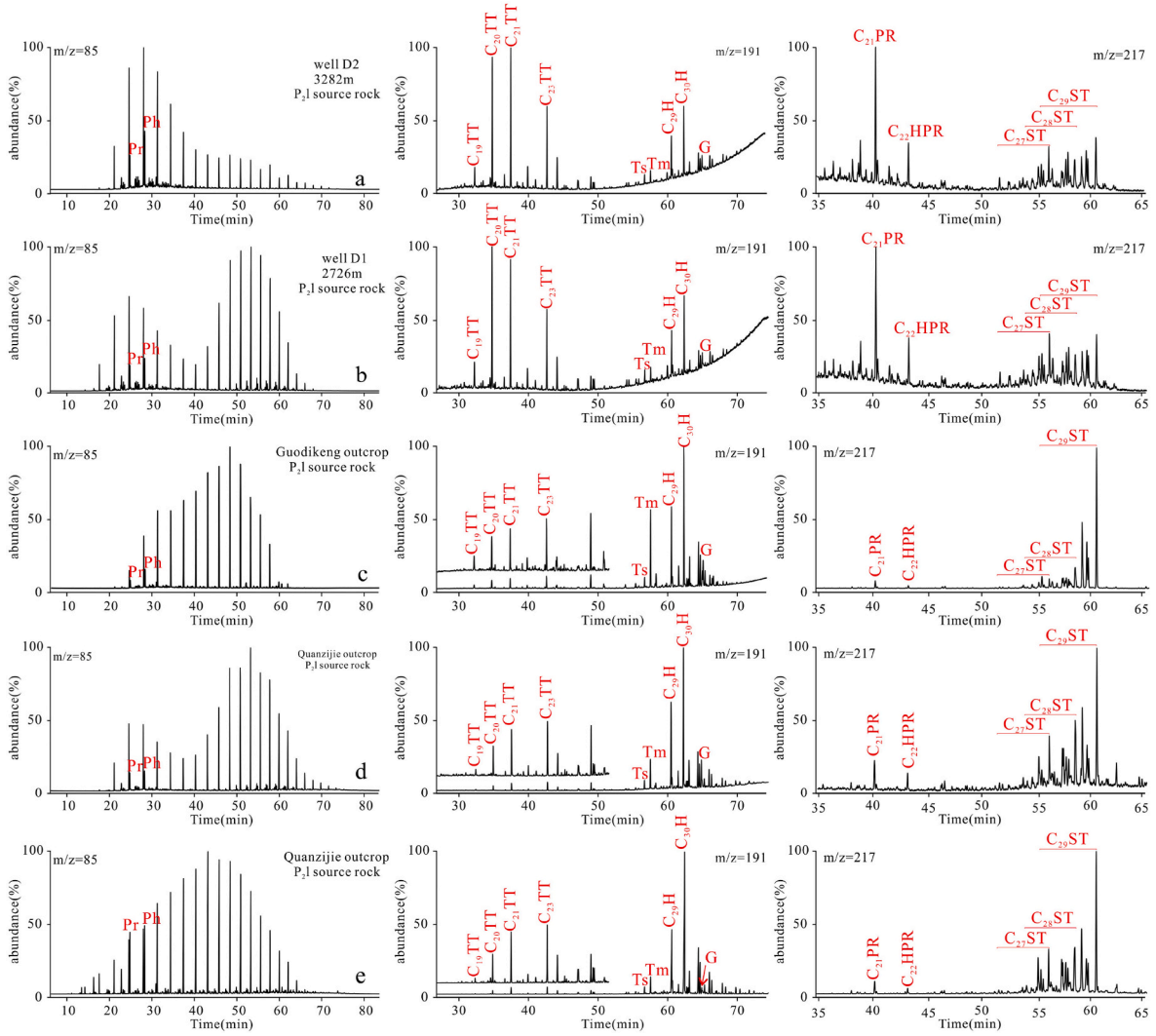

Fig. 4. Chromatograms ($m/z = 85$, $m/z = 191$, $m/z = 219$) showing the distribution characteristics of n-alkanes, terpanes and sterane of P_2l source rocks extracts from the Chaiwopu Sag and northern Bogda Mountain. Note: Pr: Pristane; Ph: Phytane; TT: tricyclic terpanes; TE: tetracylic terpanes; Ts: 18α(H),21β(H)-22,29,30-trisnorneohopane; Tm: 17α(H),21β(H)-22,29,30-trisnorhopane; H: hopane; G: gammacerane; HR: pregnane; HPR: homopregnane; ST: sterane.

Table 4
The stable carbon isotope data of source rocks and oil-sand extracts in different areas.

Well/outcrop	Depth(m)	Formation	Sample type	$\delta^{13}C$ (PDB)			
				Saturated	Aromatic	Polar compound	Asphaltene
D1	2725	P_2l	source rock	−28.0	−26.8	−27.9	−25.6
D1	2731	P_2l	source rock	−28.5	−26.3	−28.0	−26.3
D2	3052	P_2l	source rock	−28.3	−25.0	−27.6	−24.1
D2	3062	P_2l	source rock	−28.1	−26.8	−28.0	−26.1
D2	3282	P_2l	source rock	−28.2	−26.4	−27.8	−25.4
D4	3056	P_2l	source rock	−29.4	−25.8	−26.4	−25.9
D4	3057	P_2l	source rock	−28.8	−29.4	−22.5	−24.8
D4	3058	P_2l	source rock	−28.3	−25.1	−25.2	−25.5
Guodikeng	\	P_2l	source rock	−27.2	−23.4	−24.7	−21.5
Guodikeng	\	P_2l	source rock	−30.8	−25.1	−27.9	−23.8
Guodikeng	\	P_2l	source rock	−26.2	−22.3	−24.1	−21.5
Guodikeng	\	P_2l	source rock	−29.3	−26.6	−28.5	−25.8
Guodikeng	\	P_2l	source rock	−35.9		−31.6	−28.9
Quanzijie	\	P_2l	source rock	−34.0	−31.0	−31.2	−30.3
Quanzijie	\	P_2l	source rock	−34.5	−30.7	−31.0	−28.8
Quanzijie	\	P_2l	source rock	−34.3	−30.0	−30.0	−28.9
Quanzijie	\	P_2l	source rock	−34.4	−29.2	−26.8	−28.7
Quanzijie	\	P_2l	source rock	−33.7	−28.2	−29.1	−22.2
Quanzijie	\	P_2l	source rock	−31.9	−29.5	−28.8	−29.4
Quanzijie	\	P_2l	source rock	−39.9	−32.7	−34.0	−30.5
D5	200.0–230.0	P_1t	oil-sand	−26.3	−25.6	−25.2	−24.8
D6	280.0–300.0	P_1t	oil-sand	−27.3	−26.6	−26.2	−26.1
D6	320.0–330.0	P_1t	oil-sand	−34.1	−28.5	−28.0	−27.8
D7	360.0–370.0	P_1t	oil-sand	−27.9	−26.7	−26.3	−26.3

4.2. Geochemical characteristics of oil-bearing siltstone

4.2.1. Biomarker characteristics of oil-sand extraction

The TIC (total ion chromatogram) of saturated hydrocarbons in well D5 shows UCM characteristics (Fig. 5a). Except for the sample of well D6 (320.0–330.0 m) (Figs. 5c and 6c), the *n*-alkanes in other samples were partially destroyed and the C_{29}-25-norhopane was detected (Fig. 6a, b and 6d). Terpane compounds including tricyclic, tetracyclic terpanes and pentacyclic triterpenes were detected in these oil-sand extracts that were analyzed in this study (Fig. 6a, b, d). In addition, hopanes in the sample of well D7 has been partially destroyed (Fig. 6d). Except for the sample of well D7 (Fig. 7d), the steranes including pregnane, regular sterane and rearranged sterane series were detected in other samples (Fig. 7a, b and 7c). The C_{27}-rearranged steranes have been partially destroyed in the sample of well D5, but the highly abundant $C_{27\text{-}29}$-regular steranes is still detected (Fig. 7a). Furthermore, the regular sterane and rearranged sterane series have been destroyed in the sample of well D7 (Fig. 7d).

The C_{29}ααα20S/(20S + 20R) and C_{29}αββ/(αββ+ααα) ratios for oil-sand extract of well D6 (320.0–330.0m) are 0.46 and 0.43, and those ratios for oil-sand extract of well D6 (280.0–300.0m) are 0.49 and 0.51, respectively (Table 5). The C_{27}/C_{29}-ST and C_{28}/C_{29}-ST ratios are 0.64 and 0.65 in the oil-sand extract of well D6 (320.0–330.0m), respectively (Table 5). Other biomarker parameters are shown in Table 5.

According to the biodegradation level of crude oil proposed by Peters and Moldowan (1993), the crude oil has undergone different degrees of biodegradation in the eastern Chaiwopu Sag, ranging from PM 1 to PM 9. The distribution of *n*-alkanes, terpane compounds and steranes is complete and C_{29}-25-norhopane is not detected in oil-sand extract of well D6 (320.0–330.0 m), indicating that the oils underwent light biodegradation (PM level 1). The distribution of steranes is complete and C_{29}-25-norhopane is detected in oil-sand extract of well D6 (280.0–300.0m), indicating that the oils underwent moderate biodegradation (PM level 5). The distribution of *n*-alkanes and C_{27}-rearranged steranes is alterative and C_{29}-25-norhopane is detected in oil-sand extract of well D5, indicating that the oils underwent heavy biodegradation (PM level 6 or 7). The distribution of *n*-alkanes, terpanes and steranes is alterative and C_{29}-25-norhopane is detected in oil-sand extract of well D7, indicating that the oils underwent very strong biodegradation (PM level 9).

However, the *n*-alkanes were detected in moderately degraded oil, heavily degraded oil and very strongly degraded oil, indicating there are two or more stages of hydrocarbon charging in the eastern Chaiwopu Sag. It is speculated that the *n*-alkanes in the crude oils formed during the first charging stage of wells D5, D6 (280.0–300.0 m) and D7 have been totally degraded, and current *n*-alkanes mainly reflect the characteristics of the crude oils formed during the second charging stage. The distribution characteristics of terpanes and steranes mainly reflect the mixed oil characteristics of wells D5, D6 (280.0–300.0 m) and D7.

Heavy biodegradation resulted in heavy destruction of steranes in the crude oil of wells D5 and D7 (Fig. 7a and d). The steranes of crude oil from well D5 reflect the characteristics of mixed oil, which are discussed above. Comparing the maturity of lightly degraded oil and moderately degraded oil, it shows that the maturity of two stages of crude oil is different, one of which has a low maturity and the other has a high maturity. For slightly degraded crude oil, the parameters related to steranes can still reflect the geochemical characteristics of crude oil and its corresponding source rocks. The C_{27}/C_{29}-ST and C_{28}/C_{29}-ST ratios of the lightly degraded oil (D6, 320.0–330.0 m) indicate that the organisms of corresponding source rocks are a mixture of terrigenous and aquatic.

4.2.2. The stable carbon isotopes of oil-sand extraction

The carbon isotope oil-sand extracts are shown in Table 4. Stable carbon isotope of the biodegradable oil-sand extraction group are as follows: $\delta^{13}C_{saturated} < \delta^{13}C_{aromatic} < \delta^{13}C_{polar\ compounds} \leq \delta^{13}C_{asphaltenes}$, indicating the stable carbon isotope values are not affected by biodegradation in the eastern Chaiwopu Sag (Stahl., 1978). As a result, the stable carbon isotope values can be used for oil-oil and oil-source correlations of biodegraded crude oil in the study area (Sofer, 1984; Galimov, 2006; Pehlivanli et al., 2014; Sun et al., 2019).

The values of stable carbon isotope indicate that there are two crude oil populations. One of the crude oil populations is characteristic of relatively abundant light carbon isotopes (D6, 320.0–330.0 m) (Table 4), while the other is relatively rich in heavy carbon isotopes (wells D5, D7 and D6 (280.0–300.0 m)) (Table 4). In addition, the saturated hydrocarbons of oil-sand extracts have relatively light carbon isotopes (Table 4), which is similar to the P_2l source rocks in the Chaiwopu Sag and the northern Bogeda Mountains.

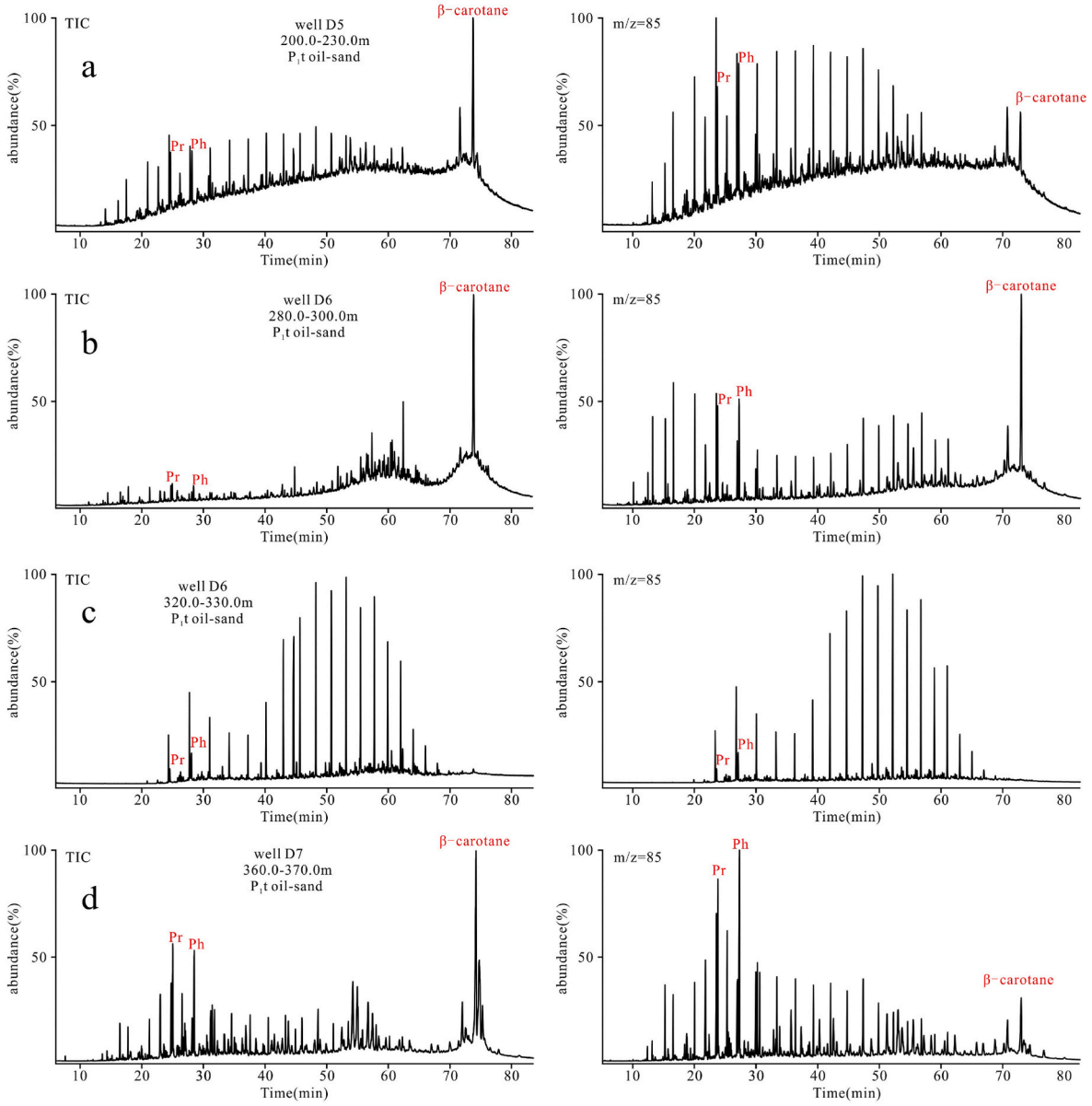

Fig. 5. Chromatograms (*TIC*, *m/z* = 85) showing the distribution characteristics of n-alkanes of P_1t oil-sand extracts from the eastern Chaiwopu Sag (refer to Fig.4 for an explanation of the abbreviations).

4.2.3. The petrographic characteristics of hydrocarbon inclusions

The fluorescence characteristics of hydrocarbon inclusions are an important feature that distinguishes them from other fluid inclusions (Stasiuk and Snowdon, 1997). With the maturity evolution of organic matter from low to high, the fluorescence compounds increase gradually and phases of hydrocarbon in inclusions change from liquid to gas (Zhao et al., 2019). In response to the changes in maturity, the color and fluorescence properties of hydrocarbon in inclusions also change regularly. The color of hydrocarbon in inclusions changes from dark, yellow to colorless, and the fluorescence changes from dark, yellow to blue (Goldstein, 2001). Therefore, scholars often use the color and fluorescence properties of hydrocarbon inclusions to study the maturity of hydrocarbons (Hagemann and Hollerbach, 1986; Videtich et al., 1988; George et al., 2001; Zhao et al., 2019).

There are a lot of hydrocarbon inclusions in the Tashikula Formation (P_1t) reservoirs in the eastern Chaiwopu Sag. Previous studies show that the main diagenetic sequences of the P_2l in the study area are as follows: compaction, cementation of micritic calcite, quartz, cementation of zeolite, acidic organic fluid charging, dissolution, authigenic clay precipitation and cementation of sparry calcite (Li, 2006). Analysis of petrographic characteristics of hydrocarbon inclusions reveals that there are two periods of hydrocarbon inclusions in the P_1t reservoirs (Table 6).

The period I hydrocarbon inclusions are distributed in the pore space-filled calcite (Fig. 8a and c), with a diameter of 2–15 μm. These hydrocarbon inclusions are primary inclusions formed after dissolution and appear yellow or brown under polarized light. They are mainly liquid-phase hydrocarbon inclusions, but gas-phase hydrocarbon inclusions were also observed. The gas-liquid ratio of the hydrocarbon inclusions is less than 10%. These hydrocarbon inclusions show yellow or yellow-brown fluorescence (Fig. 8b and d).

The period II hydrocarbon inclusions are distributed along the calcite veins (Fig. 8e and g) and have a diameter of 5–18 μm. These hydrocarbon inclusions are primary inclusions formed during the cementation of sparry calcite and appear faint yellow-faint brown under polarized light. The period II hydrocarbon inclusions are composed of liquid-phase hydrocarbon inclusions and gas-phase hydrocarbon inclusions. The gas-liquid ratio of the hydrocarbon inclusions is less than 10%. These hydrocarbon inclusions show blue fluorescence (Fig. 8f and h).

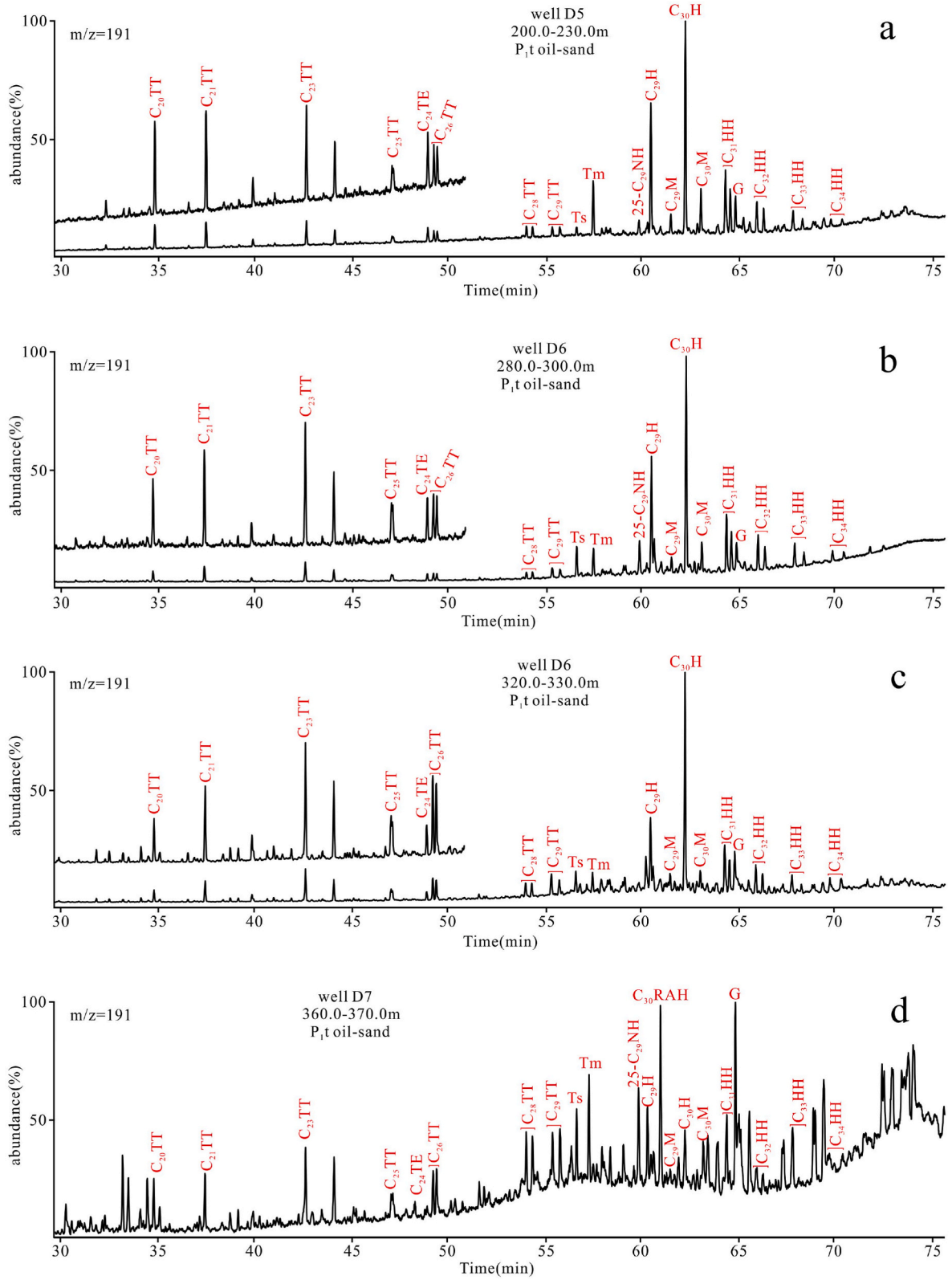

Fig. 6. Chromatograms (m/z = 191) showing the distribution characteristics of terpanes of P_1t oil-sand extracts from the eastern Chaiwopu Sag. Note: NH: norhopanes; RAH: rearrangement hopanes; M: moretane, refer to Fig.4 for other explanations of the abbreviations.

The petrographic characteristics of the P_1t hydrocarbon inclusions reflect that the study area records two periods of hydrocarbon charging. The yellow or yellow-brown fluorescence properties of the period I hydrocarbon inclusions show that the maturity of hydrocarbons formed during the first stage is low, and blue fluorescence properties of the period II hydrocarbon inclusions show that the maturity of hydrocarbons formed during the second charging stage is relatively high. Only the period I hydrocarbon inclusions developed in well D6 (320.0–330.0), and the crude oil is basically non-biodegradation. Thus, we believe that the crude oil of well D6 (320.0–330.0) represents the

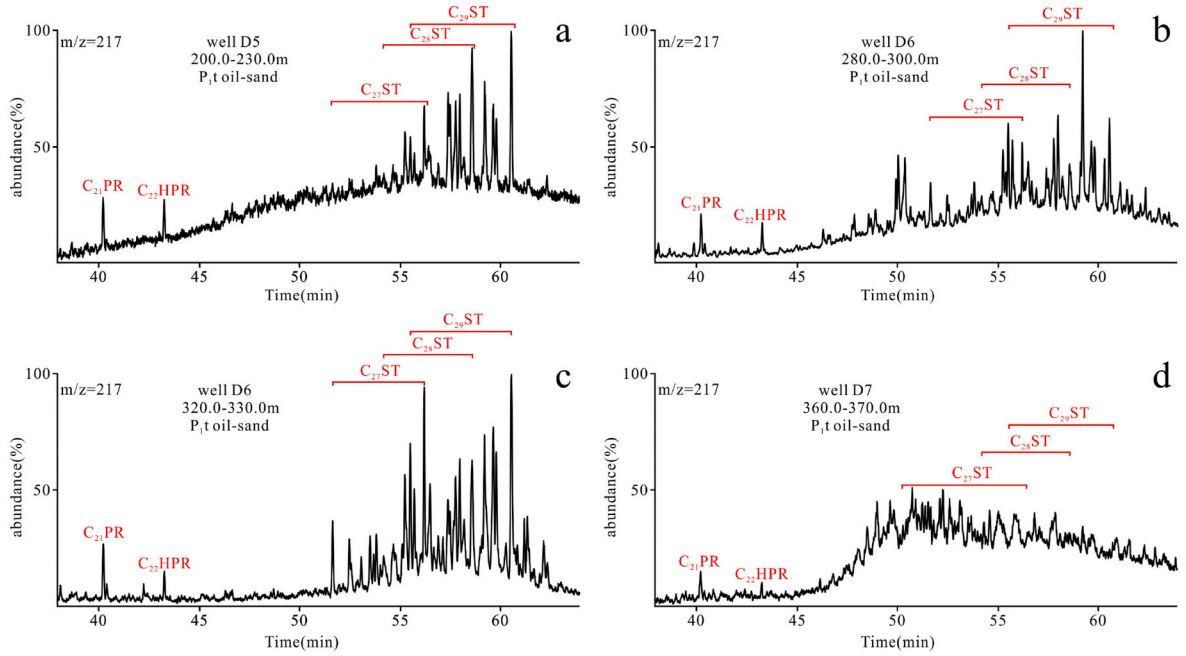

Fig. 7. Chromatograms ($m/z = 217$) showing the distribution characteristics of steranes of P_1t oil-sand extracts from the eastern Chaiwopu Sag (refer to Fig.4 for an explanation of the abbreviations).

Table 5
Some biomarker parameters of reservoir oil and hydrocarbon inclusions in the P_1t in the southeastern Chaiwopu Sag.

Well	Reservoir oil				Hydrocarbon inclusions	
	D5	D6	D6	D7	D6	D6
Depth (m)	200.0–230.0	280.0–300.0	320.0–330.0	360.0–370.0	295.0–300.0	320.0–330.0
PM	6 or 7	5	1	9	/	/
C_{23} TT/C_{21} TT	1.01	1.65	1.34	1.66	0.74	1.02
C_{23} TT/C_{20} TT	1.15	2.79	1.86	1.76	0.34	0.95
C_{24} TE/C_{26} TT	0.68	0.59	0.45	0.08	0.65	1.06
Ts/(Ts + Tm)	0.15	0.53	0.53	0.41	0.62	0.48
C_{31}–22S/(22S + 22R) HH	0.62	0.60	0.60	0.76	0.57	0.57
G/C_{30} H	0.17	0.28	0.14	2.56	0.78	0.59
ST/H	0.18	0.12	0.36	/	0.16	0.08
$C_{21\text{-}22}$ PR/$C_{27\text{-}29}$ RST	0.07	0.09	0.04	/	0.22	0.18
$C_{27\text{-}29}$ DST/$C_{27\text{-}29}$ RST	0.10	0.35	0.29	/	/	/
C_{27} RST/C_{29} RST	0.35	0.92	0.64	/	0.36	0.39
C_{28} RST/C_{29} RST	1.07	0.91	0.65	/	0.35	0.44
C_{29} STααα20S/(20S + 20R)	0.42	0.49	0.46	/	0.57	0.47
C_{29} STαββ/(αββ+ααα)	0.37	0.51	0.43	/	0.45	0.40

Table 6
The petrographic characteristics of hydrocarbon inclusions in the P_1t reservoir, in the southeastern Chaiwopu Sag.

Well	Stage	Depth (m)	Location	Gas-liquid ratio (%)	Color under polarized light	Color under fluorescent light
D5	I	200.0–210.0	dissolution pore	≤5	yellow, brown	yellow, yellow-brown
	II	220.0–225.0	calcite vein	10	faint yellow-faint brown	blue
D6	I	280.0–290.0	dissolution pore	5–10	yellow, brown	yellow
	II	295.0–300.0	calcite vein	\	faint yellow-faint brown	blue
D6	I	320.0–330.0	dissolution pore	≤5	yellow, brown	yellow, yellow-green
D7	II	360.0–365.0	calcite vein	≤5	faint yellow-faint brown	blue

hydrocarbons formed during the first charging stage with low maturity.

4.2.4. The geochemical characteristics of hydrocarbon in inclusions

According to the results of petrographic analysis, the well D6 oil-bearing sandstone samples were selected for the analysis of geochemical characteristics of hydrocarbon in inclusions. The sample at the depth 320.0–330.0 m represents the first charging stage, and the sample at the depth of 295.0–300.0 m represents the second charging stage (Table 6).

The biomarker characteristics of hydrocarbons in inclusions are shown in Fig. 9. The content of short-chain *n*-alkanes is high in the first charging stage and the second charging stage. The relative abundance of $C_{20\text{-}23}$ tricyclic terpanes show the characteristics of $C_{23} > C_{21} > C_{20}$ in the period I hydrocarbon inclusions, while the period II hydrocarbon inclusions show the characteristics of $C_{23} < C_{21} < C_{20}$. The Ts/(Ts + Tm), C_{29}ααα20S/(20S + 20R) and C_{29}αββ/(αββ+ααα) values are 0.48, 0.47

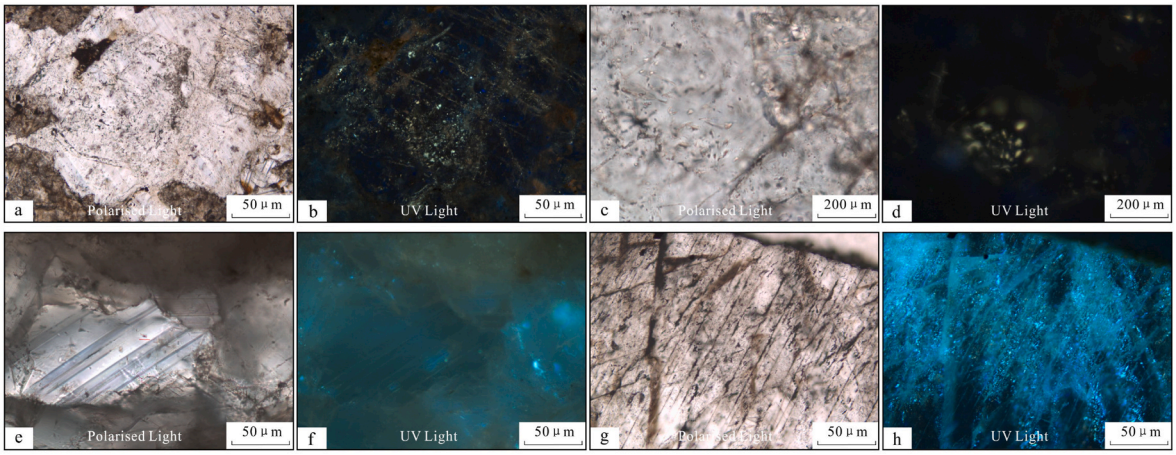

Fig. 8. Microscopic characteristics of hydrocarbon inclusions in the Tashikula Formation reservoir, in the eastern Chaiwopu Sag. (a–b) hydrocarbon inclusions distributed in the pore space-filled calcite, which fluoresce yellow and brown, well D6, depth 320.0–330.0 m; (c–d) hydrocarbon inclusions distributed in the pore space-filled calcite, which fluoresce yellow, well D6, depth 320.0–330.0 m; (e–f) hydrocarbon inclusions distributed along the calcite veins, which fluoresce blue, well D5, depth 220.0–230.0 m; (g–h) hydrocarbon inclusions distributed along the calcite veins, which fluoresce blue, well D7, depth 360.0–370.0 m. (For interpretation of the references to color in this figure legend, the reader is referred to the Web version of this article.)

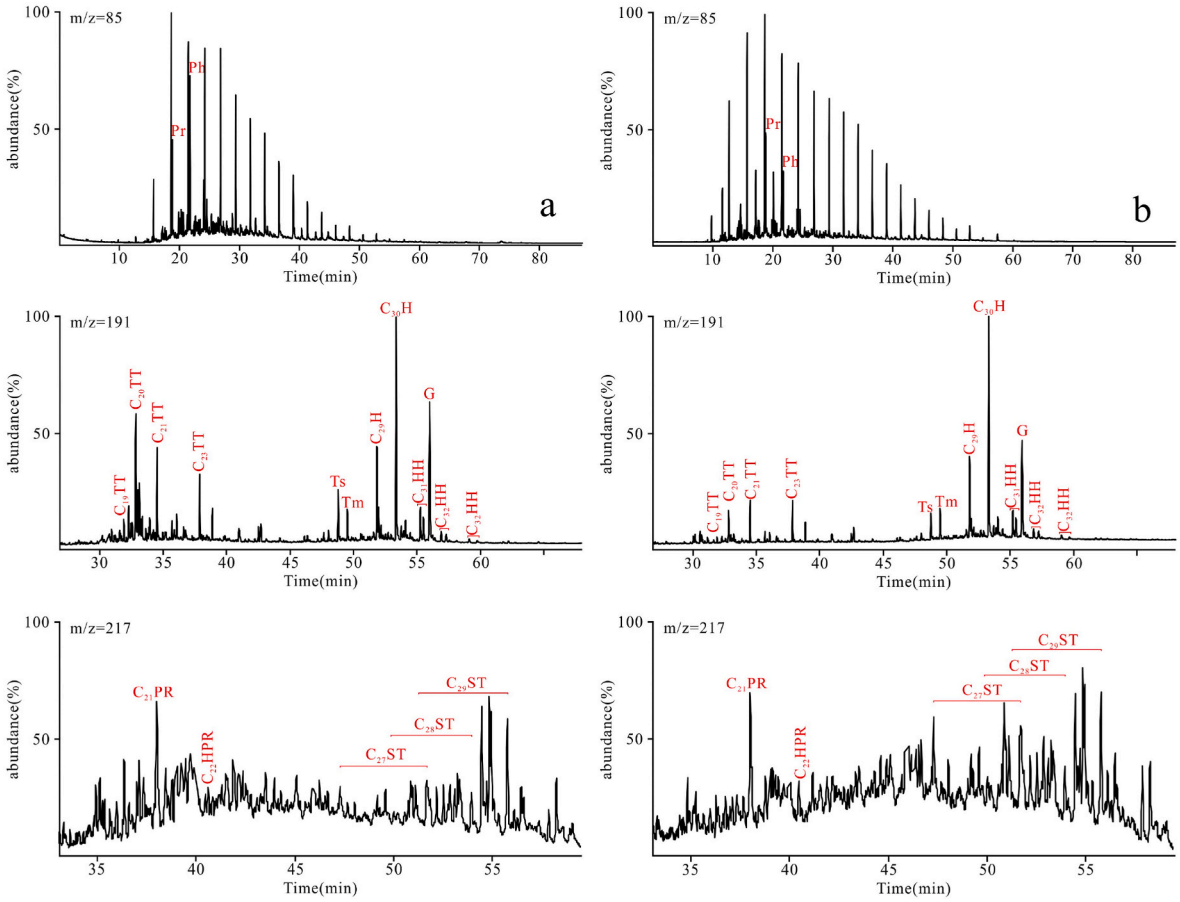

Fig. 9. Chromatograms (m/z = 85, m/z = 191, m/z = 217) showing the distribution characteristics of n-alkanes, terpanes and steranes of P_1t hydrocarbon inclusions, in the eastern Chaiwopu Sag (Left: well D6, 295.0–300.0 m; Right: well D6, 320.0–330.0 m. Refer to Fig.4 for an explanation of the abbreviations).

and 0.40 in the period I hydrocarbon inclusions, and these values in the period II hydrocarbon inclusions are 0.62, 0.57 and 0.45 (Table 5). In addition, the G/C_{30} H values of the period I hydrocarbon inclusions and the period II hydrocarbon inclusions are 0.59 and 0.78 (Table 5), respectively. Other biomarker parameters are shown in Table 5.

The distribution of *n*-alkanes, terpanes and steranes is basically complete in the period I hydrocarbon inclusions and the period II hydrocarbon inclusions (Fig. 9), indicating that the crude oil whether filling in the first charging stage or in the second charging stage did not undergo biodegradation when they are captured by inclusions. The biodegradation of crude oil in the reservoir is mainly caused by the deterioration of geological conditions in the later stage. Comparing

biomarker characteristics of C_{20-23} tricyclic terpanes in the two periods hydrocarbon inclusions, it also shows that there are two crude oil populations in the P_1t reservoirs. Biomarker maturity parameters of the two periods hydrocarbon inclusions indicate that hydrocarbons formed during the first charging stage is characterized by low maturity and hydrocarbons formed during the second charging stage is characterized by high maturity. In addition, the G/C_{30} H value of the period I hydrocarbon inclusions is lower than that of the period II hydrocarbon inclusions, indicating that the source rock corresponding to the hydrocarbon formed during the first charging stage is deposited in low salinity water, while the source rock corresponding to the hydrocarbon formed during the second charging stage is deposited in high salinity water.

4.3. Origin of oil in the eastern Chaiwopu Sag

The *n*-alkanes are rich in short-chain compounds and the abundance of the pentacyclic triterpenes is much higher than that of the tricyclic terpanes in the period I hydrocarbon inclusions (Fig. 9b), which is consistent with the P_2l shales in the outcrops of Guodikeng and Quanzijie (Fig. 4c–e). The *n*-alkanes are rich in short-chain compounds and the abundance of the tricyclic terpanes is high in the period II hydrocarbon inclusions (Fig. 9a), which is consistent with the P_2l mudstones of well D2 (Fig. 4a and b). Previous studies showed that the tricyclic terpanes are more resistant to degradation than hopanes and steranes (Peters et al., 1990). Therefore, we suggest that biomarker characteristic of C_{20-23} tricyclic terpanes should be used for oil-source correlation. The relative abundance of C_{20-23} tricyclic terpanes has the characteristics of $C_{23}> C_{21}> C_{20}$ in the period I hydrocarbon inclusions (Fig. 9b) and oil-sand extracts (Fig. 6a–c), which is consistent with the P_2l shales in the outcrops of Guodikeng and Quanzijie (Fig. 4c–e). The relative abundance of C_{20-23} tricyclic terpanes has the characteristics of $C_{23}< C_{21}< C_{20}$ in the period II hydrocarbon inclusions (Fig. 9a), which is consistent with the P_2l mudstones of well D1 (Fig. 4b).

The saturated and aromatic hydrocarbons of the slightly biodegraded oil (well D6, P_1t, 320.0–330.0 m) are relatively rich in light carbon isotopes, which is consistent with the P_2l shales in the Quanzijie outcrop (Fig. 10). The saturated and aromatic fractions of other oils are relatively rich in heavy carbon isotopes, which is consistent with the P_2l mudstones and shales in the wells D1, D2, D4 and the Guodikeng outcrop (Fig. 10).

Based on the above analysis, we infer that the hydrocarbons formed during the first charging stage originated from the P_2l shales in the northern Chaiwopu Sag and the northern Bogeda Mountains, and the hydrocarbons formed during the second charging stage originated from the P_2l mudstones in the central Chaiwopu Sag. This is basically consistent with the tectonic evolution of the Chaiwopu Sag. During the Middle Permian, affected by the paleo-uplift of the Tianshan Mountains, the middle and south of the Chaiwopu Sag were located at the fan delta and lacustrine sedimentary system against the background of a lacustrine transgression system tract, and the depocenter of the Lucaogou Formation was located in the Bogeda Mountains area. The multi-stage superimposed fan delta front sand body extends to the sedimentary central of the Lucaogou Formation from south to north (Bogeda Mountains area), which forms the channel of petroleum migration from north to south. After the Late Jurassic, the eastern Chaiwopu Sag rapidly uplifted under the influence of the Bogeda Mountains uplift, forming the current structural framework of high in the east and low in the middle of the Chaiwopu Sag. Faults form the channel of petroleum migration from the middle to the east of the Chaiwopu Sag. Furthermore, the P_2l high-quality source rocks are deposited in the surrounding area of Bogeda Mountains, and the P_2l high-quality reservoirs are deposited in the southern Bogeda Mountains (Li, 2006; Zhou et al., 2020). Therefore, the northern Chaiwopu Sag has a significant exploration potential of tight/shale oil.

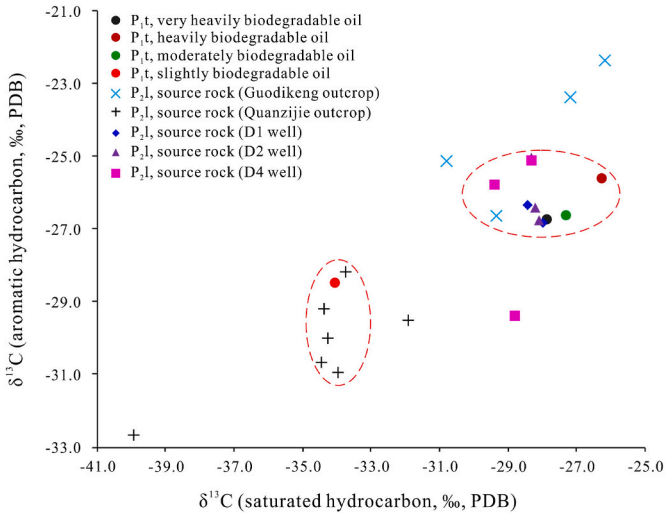

Fig. 10. Carbon isotope distribution characteristics of extracts from oil-sad and potential source rocks in the Chaiwopu Sag and northern Bogda Mountains.

5. Conclusions

Affected by tectonic movement, the oil in the eastern Chaiwopu Sag has undergone different degrees of biodegradation, ranging from PM 1 to PM 9. Ordinarily, biomarkers and isotopes were mainly used for oil-source correlation analysis, but some molecular parameters of degraded oil were distorted in the study area. In this study, we analyzed the geochemical characteristics of degraded oil through hydrocarbon inclusions, which provides a new tool for oil-source correlation study under complex geological conditions.

The characteristics of biomarkers and carbon isotopes of crude oil, petrographic and biomarkers characteristics of hydrocarbon inclusions all indicate that there are two crude oil populations in the P_1t reservoirs. The hydrocarbon formed during the first charging stage has lower maturity and relatively light carbon isotope composition, its C_{20-23} tricyclic terpanes show the characteristics of $C_{23}> C_{21}> C_{20}$. The hydrocarbon formed during the second charging stage has higher maturity and relatively heavy carbon isotope composition, and the abundance of C_{20-23} tricyclic terpanes is characterized by $C_{23}<C_{21}< C_{20}$.

The biomarkers and isotope characteristics of crude oil, potential source rocks and hydrocarbon inclusions reveal that hydrocarbons formed during the first charging stage originated from the P_2l source rocks in the northern Chaiwopu Sag and the northern Bogeda Mountains, hydrocarbons formed during the second charging stage originated from the P_2l source rocks in central Chaiwopu Sag. The P_2l high-quality source rocks and reservoirs are deposited in the northern Chaiwopu Sag, which has great potential for tight/shale oil exploration.

Author statement

Ruihui Zheng: Conceptualization, Writing – original draft, Resources. Guanlong Zhang: Supervision, Writing – review & editing. Yansheng Qu: Validation, Resources. Investigation, Resources. Shengzhu Wang: Investigation, Resources. Xiao Jin: Investigation. Xue Chen: Investigation. Zhihuan Zhang: Supervision, Funding acquisition.

Declaration of competing interest

The authors declare that they have no known competing financial interests or personal relationships that could have appeared to influence the work reported in this paper.

References

Alizadeh, B., Maroufi, K., Fajrak, M., 2018. Oil-oil correlation, geochemical characteristics, and origin of hydrocarbonsfrom Mansourabad oilfield, SW Iran. J. Afr. Earth Sci. 147, 383–392.

Aplin, A.C., Macleod, G., Larter, S.R., Pedersen, K.S., Sorensen, H., Booth, T., 1999. Combined use of Confocal Laser Scanning Microscopyand PVT simulation for estimating the composition andphysical properties of petroleum in fluid inclusions. Mar. Petrol. Geol. 16, 97–110.

Duschl, F., Kerkhof, A.V.D., Sosa, G., Leiss, B., Wiegand, B., Vollbrecht, A., Sauter, M., 2016. Fluid inclusion and microfabric studies on Zechstein carbonates (Ca2) and related fracture mineralizations – new insights on gas migration in the Lower Saxony Basin (Germany). Mar. Petrol. Geol. 77, 300–322.

Fan, J.T., 2018. Study on Organic Geochemical Characteristics of Permian Argillaceous Shale and Formation Conditions of Shale Gas in Chaiwopu Sag. Chang'an University, Xi'an (In Chinese with English abstract).

Galimov, E.M., 2006. Isotope organic geochemistry. Org. Geochem. 37 (10), 1200–1262.

George, S.C., Ruble, T.E., Dutkiewicz, A., Eadington, P.J., 2001. Assessing the maturity of oil trapped in fluid inclusions using molecular geochemistry data and visually-determined fluorescence colours. Appl. Geochem. 16, 451–473.

Goldstein, R.H., 2001. Fluid inclusions in sedimentary and diagenetic systems. Lithos 55, 159–193.

Gratzer, R., Bechtel, A., Sachsenhofer, R.F., Linzer, H.G., Reischenbacher, D., Schulz, H. M., 2011. Oil-oil and oil-source rock correlations in the Alpine Foreland Basin of Austria:Insights from biomarker and stable carbon isotope studies. Mar. Petrol. Geol. 28, 1171–1186.

Guo, Y.Q., 1997. Geochemical characteristic and genetic type of oils in Chaiwopu sag. Xinjing Pet. Geol. 1, 59–68 (In Chinese with English abstract).

Guo, J.J., Zhu, Z.Y., Li, G.C., Chen, J.F., Chen, Z.Y., 2004. The geochemistry characteristics of source rock in well Chaican 1 ce 1 in Chaiwopu Sag. Natural Gas Geoscience 15 (6), 652–654 (In Chinese with English abstract).

Guo, J.J., Chen, J.F., Zhu, Z.Y., Chen, Z.Y., Xiao, J.B., 2006. Geochemical characteristics of upper permian source rocks and exploration directions in Dabancheng sub-depression of Chaiwopu depression. Acta Sedimentol. Sin. 3, 446–455 (In Chinese with English abstract).

Hagemann, H.W., Hollerbach, A., 1986. The fluorescence behaviour of crude oils with respect to their thermal maturation and degradation. Org. Geochem. 10, 473–480.

Hu, T., Pang, X.Q., Jiang, S., Wang, Q.F., Zheng, X.W., Ding, X.G., Zhao, Y., Zhu, C.X., Li, H., 2018. Oil content evaluation of lacustrine organic-rich shale with strongheterogeneity: a case study of the Middle Permian Lucaogou Formation inJimusaer Sag, Junggar Basin, NW China. Fuel 221, 196–205.

Körmös, S., Schsenhofer, R.F., Bechtel, A., Radovics, B.G., Milota, K., Schubert, F., 2021. Source rock potential, crude oil characteristics and oil-to-source rock correlation in a Central Paratethys sub-basin, the Hungarian Palaeogene Basin (Pannonian basin). Mar. Petrol. Geol. 127, 104955.

Kuang, L.X., Guo, J.H., Wang, Y.M., Li, G.C., 2005. Studies on the potential of oil & gas resource in Chaiwopu depression. Journal of Southwest Petroleum University (Science & Technology Edition) 5, 15–19 (In Chinese with English abstract).

Li, H., 2006. Oil and Gas Geological Conditions Comprehensive Study in Chaiwopu Sag, Junggar Basin. Northwest University, Xi'an (In Chinese with English abstract).

Liu, K., Eadington, P., 2005. Quantitative fluorescence techniques for detecting residual oils and reconstructing hydrocarbon charge history. Org. Geochem. 36, 1023–1036.

Liu, K.Y., Eadington, P., Middleton, H., Fenron, S., Cable, T., 2007. Applying quantitative fluorescence techniques to investigate petroleum charge history of sedimentary basins in Australia and Papuan New Guinea. J. Petrol. Sci. Eng. 57, 139–151.

Mashhadi, Z.S., Rabbani, A.B., 2015. Organic geochemistry of crude oils and Cretaceous source rocks in theIranian sector of the Persian Gulf: an oil–oil and oil–source rock correlation study. Int. J. Coal Geol. 146, 118–144.

McLimans, R.K., 1987. The application of fluid inclusions to migration of oil and diagenesis in petroleum reservoirs. Appl. Geochem. 2, 585–603.

Parnell, J., Middleton, D., Chen, H.H., Hall, D., 2001. The use of integrated fluid inclusions studies in constraining oil charge history and reservoirs compartmentation: examples from the Jeanne d'Arc Basin, offshore Newfoundland. Mar. Petrol. Geol. 18, 535–549.

Pehlivanli, B.Y., Koç, Ş., Sari, A., 2014. Carbon isotope ($\delta^{13}C$) characteristics of middle Miocene Çayirhan oil shales (Beypazari, Ankara/Turkey): implications on paleoenvironment and paleoclimate. Fuel 135, 427–434.

Peters, K.E., 1986. Guidelines for evaluating petroleum source rock using programmed pyrolysis. AAPG (Am. Assoc. Pet. Geol.) Bull. 70 (3), 318–329.

Peters, K.E., Moldowan, J.M., Sundararaman, P., 1990. Effects of hydrous pyrolysis on biomarker thermal maturity parameters: monterey Phosphatic and Siliceous members. Org. Geochem. 15, 249–265.

Peters, K.E., Moldowan, J.M., 1993. The Biomarker Guide: Interpreting Molecular Fossils in the Petroleum and Ancient Sediments. Prentice Hall, Englewood Cliffs, N, J.

Peters, K.E., Walters, C.C., Moldowan, J.M., 2005. The Biomarker Guide, second ed. Cambridge University Press, New York.

Pironon, J., 2004. Fluid Inclusions in Petroleum Environments: Analytical Procedure for PTX Reconstruction.

Ruble, T.E., George, S.C., Lisk, M., Quezada, R.A., 1998. Organic compounds trapped in aqueous fluid inclusions. Org. Geochem. 29, 195–205.

Ryder, A.G., Przyjalgowski, M.A., Feely, M., Szczupak, B., Glymn, T.J., 2004. Timeresolved fluorescence microspectroscopy for characterizing crude oils in bulk and hydrocarbon bearing fluid inclusions. Appl. Spectrosc. 58, 1106–1115.

Seifert, W.K., Moldowan, J.M., Demaison, G.J., 1984. Source correlation of biodegraded oils. Org. Geochem. 6, 633–643.

Stahl, W.J., Carey, B.D., 1975. Source-rock identification by isotope analyses of natural gases from fields in the Val Verde and Delaware basins, west Texas. Chem. Geol. 16 (4), 257–267.

Stasiuk, L.D., Snowdon, L.R., 1997. Fluorescence micro-spectrometry of synthetic and natural hydrocarbon fluid inclusions: crude oil chemistry, density and application to petroleum migration. Appl. Geochem. 12 (3), 229–241.

Sofer, Z., 1984. Stable carbon isotope compositions of crude oils: application to source depositional environments and petroleum alteration. AAPG (Am. Assoc. Pet. Geol.) Bull. 68 (1), 31–49.

Sun, Q.S., Xiao, F., Gao, X.Y., Zong, W.M., Li, Y.F., Zhang, J., Sun, S.L., Chen, S.W., 2019. A new discovery of Mesoproterozoic erathem oil, and oil–source correlation in the Niuyingzi area of western Liaoning Province, NE China. Mar. Petrol. Geol. 110, 606–620.

Thiéry, R., Pironon, J., Walgenwitz, F., Montel, F., 2002. Individual characterization of petroleum fluid inclusions (composition and P–T trapping conditions) by microthermometry and confocal laser scanning microscopy: inferences from applied thermodynamics of oils. Mar. Petrol. Geol. 19, 847–859.

Tseng, H.Y., Pottorf, R.J., 2003. The application of fluid inclusion PVT analysis to studies of petroleum migration and reservoirs. J. Geochem. Explor. 78 (79), 433–436.

Videtich, P.E., McLimans, R.K., Watson, H.K.S., Nagy, R.M., 1988. Depositional, diagenetic, thermal, and maturation histories of cretaceous mishrif formation, Fateh field, Dubai. AAPG (Am. Assoc. Pet. Geol.) Bull. 72, 1143–1159.

Volk, H., Mann, U., Burde, O., Horsfield, B., Suchú, V., 2000. Petroleum inclusions and residual oils: constraints for deciphering petroleum migration. J. Geochem. Explor. 71, 307–311.

Volk, H., George, S.C., 2019. Using petroleum inclusions to trace petroleum systems – a review. Org. Geochem. 129, 99–123.

Wenger, L.M., Davis, C.L., Isaksen, G.H., 2002. Multiple controls on petroleum biodegradation and impact on oil quality. SPE Reservoir Eval. Eng. 5 (5), 375–383.

Wu, G.H., Ba, X.E., Feng, Y.H., Yang, F., Lei, J.B., 2003. Petroleum Characteristics and Prospecting Target in Chaiwopu Seg, Junggar Basin, vol. 6. Xinjiang Petroleum Geology, pp. 523–526 (In Chinese with English abstract).

Wu, X.Q., Liu, Q.Y., Chen, Y.B., Zhai, C.B., Ni, C.H., Yang, J., 2020. Constraints of molecular and stable isotopic compositions on the origin of natural gas from Middle Triassic reservoirs in the Chuanxi large gas field, Sichuan Basin, SW China. J. Afr. Earth Sci. 204, 104589.

Zhao, S.F., Chen, W., Zhou, L., Zhou, P., Zhang, J., 2019. Characteristics of fluid inclusions and implications for the timing of hydrocarbon accumulation in the cretaceous reservoirs, Kelasu Thrust Belt, Tarim Basin, China. Mar. Petrol. Geol. 99, 473–487.

Zhu, Y.M., 1997. Geochemical characteristics of terrestrial oils of the Tarim Basin. Acta Sedimentol. Sin. 15 (2), 26–30 (In Chinese with English abstract).

Zumberge, J.E., 1987. Prediction of source rock characteristics based on terpane biomarkers in crude oils: a multivariate statistical approach. Geochem. Cosmochim. Acta 51 (6), 1625–1637.